THE EFFECT OF TEMPERATURE ON TRAP-ASSISTED AND DIRECT TUNNELLING CURRENTS

Juraj Racko, Peter Benko, Miroslav Mikolášek,
Alena Grmanová, Ladislav Harmatha, Juraj Breza

Slovak University of Technology, Bratislava, Slovakia
E-mail: juraj.breza@stuba.sk

Received 27 April 2016; accepted 13 May 2016

1. Motivation

The total current flowing through the semiconductor heterostructure consists of thermionic-diffusion-drift and tunnelling components as shown in Figs. 1a and 1b. The tunnelling component stems from direct and trap-assisted tunnelling (TAT). The contributions of single types of currents vary with temperature. In this paper we have focused on comparing the temperature dependences of the two types of tunnelling currents in a real metal/GaN/AlGaN heterostructure used in the production of various types of sensors.

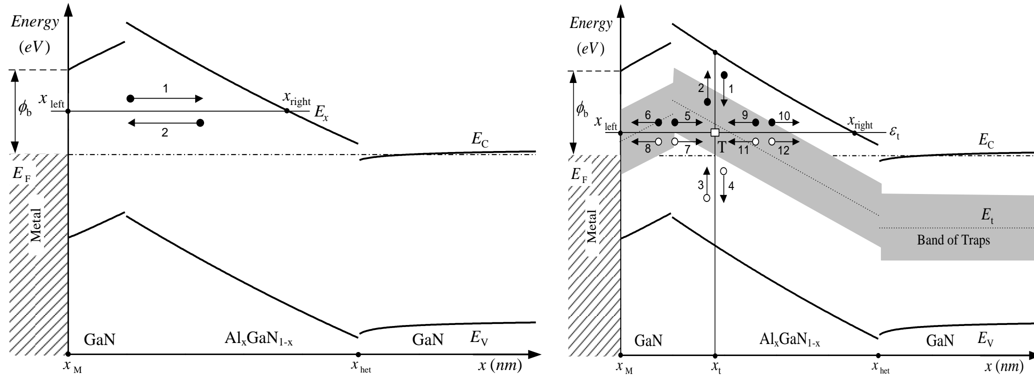

Fig. 1: *Direct tunnelling (left) and trap-assisted tunnelling (right) in a metal/*GaN/Al_XGaN_{1-X}/GaN *heterostructure. Twelve exchange processes are considered in the model of TAT. The arrows show the transitions of electrons or holes to or from the trap.*

2. Direct tunnelling current

The electron direct tunnelling current density is calculated as [1]

$$J^{e}_{DT}(x_M)=q\frac{m^{e}_{R}}{2\pi^2\hbar^3}\int_{E_c(x_{het})}^{E_c(x_M)}\Gamma^{e}(E_x)\int_0^{\infty}\left(f^{e}_{FD}(x_{left})-f^{e}_{FD}(x_{right})\right)\mathrm{d}E_{\perp}\,\mathrm{d}E_x, \quad (1)$$

where f^{e}_{FD} is the Fermi-Dirac distribution function

$$f^{e}_{FD}(x_{right/left})=1\Big/\left(1+\exp\left(\frac{E_x+E_{\perp}-E^{e}_{F}(x_{right/left})}{kT}\right)\right) \quad (2)$$

and E_F^{e} is the electron Fermi quasi level. The total energy E of the tunnelling electron between points $x_M \equiv x_{left}$ and x_{right} is $E=E_x+E_{\perp}$. Here $E_{\perp}$ is the electron energy in the direction perpendicular to the direction of transport and E_x is the electron energy in the direction of transport. Γ_e is the tunnelling probability which depends on the of electron energy in the direction of transport E_x and in WKB approximation can be written as

$$\Gamma^{\mathrm{e}}(E_{\mathrm{x}}) = \exp\left(-\frac{\sqrt{8 m_{\mathrm{T}}^{\mathrm{e}}}}{\hbar} \int_{x_{\mathrm{right}}}^{x_{\mathrm{M}}} \sqrt{E_{\mathrm{c}}(x) - E_x}\,\mathrm{d}x \right) \qquad (3)$$

because the electron energy in the direction perpendicular to the transport E_x is equal to the energy of the conduction band and at the places between which tunnelling takes place it holds $E_c(x_{right})=E_c(x_{left})=E_x$. Electron energy in the direction perpendicular to the direction of transport $E_\perp$ may assume values from zero up to the value of vacuum, which can be considered infinitely large. Further m_R^e is the effective electron mass for calculating the Richardson constant.

3. Trap-assisted tunnelling current

Based on the 12-EXT model [2], the electron trap-assisted tunnelling current density is calculated as

$$J_{\mathrm{TAT}}^{\mathrm{e}}(x_{\mathrm{M}}) = q \int_{E_{\mathrm{c}}(x_{\mathrm{het}})}^{E_{\mathrm{c}}(x_{\mathrm{M}})} \int_{x_{\mathrm{right}}}^{x_{\mathrm{M}}} \left(\frac{1 - f_{\mathrm{t}}(\varepsilon_{\mathrm{t}}, x_{\mathrm{t}})}{\tau_{\mathrm{R_{right}}}^{\mathrm{e\,TUN}}(\varepsilon_{\mathrm{t}}, x_{\mathrm{t}})} - \frac{f_{\mathrm{t}}(\varepsilon_{\mathrm{t}}, x_{\mathrm{t}})}{\tau_{\mathrm{G_{right}}}^{\mathrm{e\,TUN}}(\varepsilon_{\mathrm{t}}, x_{\mathrm{t}})} \right) D_{\mathrm{t}}(\varepsilon_{\mathrm{t}}, x_{\mathrm{t}})\,\mathrm{d}x_{\mathrm{t}}\,\mathrm{d}\varepsilon_{\mathrm{t}} \qquad (4)$$

where D_t is the multiphonon distribution functions density of trapping centres. The process of tunnelling of free electrons and holes via trapping centres lying on energy level E_t is supported by interaction with phonons. Description of the interaction of an electron captured at the trapping level with multiphonons is based on the multiphonon transitions. Instead of a discrete level E_t one has to consider a band of energy levels, see Fig. 1. The probability of finding a trap at place (ε_t, x_t) in the band of energy levels is given by the multiphonon transition probability M_t which is calculated as

$$M_{\mathrm{t}}(\varepsilon_{\mathrm{t}}, x) = \frac{(\theta \mp S)^2}{(\theta^2 + z^2)^{\frac{1}{4}}} \exp\left(\sqrt{z^2 + \theta^2} - \theta \ln\left(\frac{\theta}{z} + \sqrt{1 + \left(\frac{\theta}{z}\right)^2} \right) - S(2 f_{\mathrm{B}} + 1) - \frac{\hbar\omega_0 \theta}{2kT} \right). \qquad (5)$$

Here S is the Huang-Rhys factor representing the strength of electron-phonon coupling, $\hbar\omega_0$ is the effective phonon energy, $f_B = (\exp(\hbar\omega_0 / kT) - 1)^{-1}$ is the Bose distribution function, and θ and z are abbreviations: $\theta = |\varepsilon_t - E_t| / \hbar\omega_0$, $z = 2S\sqrt{f_B(1 + f_B)}$. The sign inside the bracket in the nominator is negative for $E_c - \varepsilon_t > E_c - E_t$ and positive for $E_c - \varepsilon_t < E_c - E_t$. The multiphonon distribution functions density of trapping centres D_t belonging to the trapping level ε_t is expressed in terms of the multiphonon transition probability M_t as

$$D_{\mathrm{t}}(\varepsilon_{\mathrm{t}}, x_{\mathrm{t}}) = \frac{N_{\mathrm{t}}(x_{\mathrm{t}})}{\sqrt{2\pi} S \hbar\omega_0} M_{\mathrm{t}}(\varepsilon_{\mathrm{t}}, x_{\mathrm{t}}), \qquad (6)$$

where $N_t(x_t)$ is the trap density belonging to the primary trapping level E_t.

Further, f_t is the probability of occupation trap of electron which it is participating twelve exchange processes

$$f_{\mathrm{t}} = \frac{\frac{1}{\tau_{\mathrm{R}}^{\mathrm{eTH}}} + \frac{1}{\tau_{\mathrm{G}}^{\mathrm{hTH}}} + \frac{1}{\tau_{\mathrm{R}x_{\mathrm{right}}}^{\mathrm{eTUN}}} + \frac{1}{\tau_{\mathrm{R}x_{\mathrm{left}}}^{\mathrm{eTUN}}} + \frac{1}{\tau_{\mathrm{G}x_{\mathrm{right}}}^{\mathrm{hTUN}}} + \frac{1}{\tau_{\mathrm{G}x_{\mathrm{left}}}^{\mathrm{hTUN}}}}{\frac{1}{\tau_{\mathrm{R}}^{\mathrm{eTH}}} + \frac{1}{\tau_{\mathrm{G}}^{\mathrm{eTH}}} + \frac{1}{\tau_{\mathrm{R}}^{\mathrm{hTH}}} + \frac{1}{\tau_{\mathrm{G}}^{\mathrm{hTH}}} + \frac{1}{\tau_{\mathrm{R}x_{\mathrm{right}}}^{\mathrm{eTUN}}} + \frac{1}{\tau_{\mathrm{G}x_{\mathrm{right}}}^{\mathrm{eTUN}}} + \frac{1}{\tau_{\mathrm{R}x_{\mathrm{left}}}^{\mathrm{eTUN}}} + \frac{1}{\tau_{\mathrm{G}x_{\mathrm{left}}}^{\mathrm{eTUN}}} + \frac{1}{\tau_{\mathrm{R}x_{\mathrm{right}}}^{\mathrm{hTUN}}} + \frac{1}{\tau_{\mathrm{G}x_{\mathrm{right}}}^{\mathrm{hTUN}}} + \frac{1}{\tau_{\mathrm{R}x_{\mathrm{left}}}^{\mathrm{hTUN}}} + \frac{1}{\tau_{\mathrm{G}x_{\mathrm{left}}}^{\mathrm{hTUN}}}} \qquad (7)$$

Twelve exchange processes considered in the 12-EXT model of trap-assisted tunnelling are schematically shown in Fig. 1b. The formulae for calculating 4 thermal exchange times are given in Tab. 1 and the corresponding eight tunnelling exchange times [3] are given in Tab. 2.

Tab. 1: *Thermal electron and hole capture and emission exchange times.*

1 (↓ T)	electron thermal capture	$1/\tau_{R}^{e\,TH} = v^{e\,TH}\sigma_{t}^{e\,TH} n(x_{t})$
2 (↑ T)	electron thermal emission	$1/\tau_{G}^{e\,TH} = v^{e\,TH}\sigma_{t}^{e\,TH} N_{c}(x_{t})\exp\left((\varepsilon_{t} - E_{c}(x_{t}))/kT\right)$
3 (T)	hole thermal capture	$1/\tau_{R}^{h\,TH} = v^{h\,TH}\sigma_{t}^{h\,TH} p(x_{t})$
4 (T)	hole thermal emission	$1/\tau_{G}^{h\,TH} = v^{h\,TH}\sigma_{t}^{h\,TH} N_{v}(x_{t})\exp\left((E_{v}(x_{t}) - \varepsilon_{t})/kT\right)$

Here, symbols $\sigma_t^{e\,TH}$ and $\sigma_t^{h\,TH}$ stand for the effective trap cross-sections for thermal electron and hole capture and emission, and $v^{e,h\,TH} = \sqrt{3kT/m^{*\,e,h}}$ are thermal velocities of charge carriers with effective masses $m^{*e,h}$.

Tab. 2a: *Four tunnelling electron capture and emission exchange times.*

5 → T T ← 9	electron tunnelling capture	$\dfrac{1}{\tau_{R\,left/right}^{e\,TUN}} = \dfrac{m_{R}^{e}\sigma_{t}^{e\,TUN}}{2\pi^{2}\hbar^{3}} f_{FD}^{e}(x_{left/right})(\Delta E)^{2}\sum_{j=0}^{N}(j+1)\Gamma_{j}^{e}(x_{left/right}, x_{t}, \varepsilon_{t})$
← 6 T T 10 →	electron tunnelling emission	$\dfrac{1}{\tau_{G\,left/right}^{e\,TUN}} = \dfrac{m_{R}^{e}\sigma_{t}^{e\,TUN}}{2\pi^{2}\hbar^{3}}\left(1 - f_{FD}^{e}(x_{left/right})\right)(\Delta E)^{2}\sum_{j=0}^{N}(j+1)\Gamma_{j}^{e}(x_{left/right}, x_{t}, \varepsilon_{t})$

Here, f_{FD}^{e} is the Fermi-Dirac distribution function, see Eqn. (2). Γ_j^{e} is the tunnelling probability which is a function of electron energy in the direction of transport $E_x=\varepsilon_t-j\Delta E$ and in WKB approximation can be written as

$$\Gamma_{j}^{e}(x_{right/left}, x_{t}, \varepsilon_{t}) = \exp\left(-\frac{\sqrt{8m^{e\,TUN}}}{\hbar}\int_{x_{t}}^{x_{right/left}}\sqrt{E_{c}(x) - \varepsilon_{t} + j\,\Delta E}\,\mathrm{d}x\right). \tag{8}$$

The overall energy of the tunnelling electron E must be equal to the energy level of the trap ε_t, therefore if the electron energy E_x in the direction of transport drops by j$\Delta\, j\,\Delta E$ then the electron energy in the direction perpendicular to the direction of transport must be enlarged by the same amount $E_{\perp}=\varepsilon_t+j\Delta E$. Summation of the series terminates with the energy increment ΔE chosen by a reasonable compromise between the time of computation and calculation accuracy, when the ratio of the exponential term Γ^{e}_{j} for j=0 to N is smaller than a chosen value, e.g., $\Gamma^{e}_{j=N}/\Gamma^{e}_{j=0}<10^{-6}$.

Tab. 2b: *Four tunnelling hole capture and emission exchange times.*

7 → T T ← 11	hole tunnelling capture	$\dfrac{1}{\tau_{R\,left/right}^{h\,TUN}} = \dfrac{m_{R}^{h}\sigma_{t}^{h\,TUN}}{2\pi^{2}\hbar^{3}} f_{FD}^{h}(x_{left/right})(\Delta E)^{2}\sum_{j=0}^{N}(j+1)\Gamma_{j}^{h}(x_{left/right}, x_{t}, \varepsilon_{t})$
← 8 T T 12 →	hole tunnelling emission	$\dfrac{1}{\tau_{G\,left/right}^{h\,TUN}} = \dfrac{m_{R}^{h}\sigma_{t}^{h\,TUN}}{2\pi^{2}\hbar^{3}}\left(1 - f_{FD}^{h}(x_{left/right})\right)(\Delta E)^{2}\sum_{j=0}^{N}(j+1)\Gamma_{j}^{h}(x_{left/right}, x_{t}, \varepsilon_{t})$

In the case of holes, analogical relations can be used to calculate Γ^{h}_{j}. Here, symbols $\sigma_t^{e\,TUN}$ and $\sigma_t^{h\,TUN}$ stand for the effective trap cross-sections for the tunnelling electron and hole capture and emission.

4. Simulation

The model was employed to simulate metal/GaN/Al_XGaN_{1-X}/GaN Schottky heterostructures. The vertical geometry of the studied structure along with the concentration profile of ionized shallow donors N^{D+} is given in Tab. 4.

Tab. 3: *Vertical geometry of the simulated structure.*

	Cover GaN	Doped AlGaN	Undoped GaN	Doped GaN
Thickness (nm)	10	10	30	10
N^{D+} (cm^{-3})	-	1.35×10^{18}	-	1.35×10^{18}

A number of parameters have to be set in the simulation. The values of parameters are summarized in Tab. 5.

Tab. 4: *The values of parameters used in simulations of I-V curves.*

Parameter	symbol	magnitude	dimension
Schottky barrier height	ϕ_{b0}	0.876	eV
sheet metal-semiconductor interface charge	P_{tot}/q	5.5×10^{11}	cm^{-2}
position of the trap level	$E_c - E_t$	0.5	eV
concentration of traps	N_t	6.7×10^{17}	cm^{-3}
effective cross section of the traps for the thermal electron and hole exchange times	$\sigma_t^{e,h\ TH}$	1×10^{-14}	cm^2
effective cross section of the traps for the tunnelling electron and hole exchange times	$\sigma_t^{e,h\ TUN}$	1.5×10^{-13}	cm^2
Huang-Rhys factor	S	5.5	-
effective phonon energy	$\hbar\omega_0$	0.033	eV

The effective electron density of states N_c and the longitudinal effective electron mass in the central (gamma) valley m_e^T depend on Al concentration only weakly. For calculating the tunnelling exchange times, effective masses $m_e^R = m_e^T = 0.2\,m_0$ were used. Other parameters, such as spontaneous polarization $P^{SP}_{Al_XGa_{1-X}N}$, piezoelectric polarization $P^{PZ}_{GaN/Al_XGa_{1-X}N}$, band gap E_g and band offset ΔE_c of the compound semiconductor Al_XGaN_{1-X} depend on the concentration and distribution of aluminium in the cover GaN and in the doped Al_XGaN_{1-X} layers [4].

On applying a reverse voltage we simulated the current density at different temperatures from 250 K to 375 K with temperature step 25 K, see Fig. 2. The total current consists of three components: trap-assisted tunnelling current J^e_{TAT}, direct tunnelling current J^e_{DT}, and termionic-drift-diffusion current $J^e_{TE\text{-}DD}$. The graph shows very good agreement between the measured and simulated currents at 300 K. Figure 3 shows the simulated temperature dependence of $J^e_{TAT}(x_M)$ at the metal/GaN interface at different temperatures. Simulations reveal that at temperatures above 350 K and reverse voltages above 1.5 V the trap-assisted tunnelling current $J^e_{TAT}(x_M)$ saturates because thermal exchange processes dominate over the tunnelling exchange processes. The thermal electron capture and emission exchange times decrease with increasing temperature much more than the tunnelling exchange times. The temperature dependence of single mechanisms of charge transport is

shown in Figs. 4a,b,c. Predominance of the direct tunnelling current $J^{\mathrm{e}}_{\mathrm{DT}}(x_{\mathrm{M}})$ at higher temperatures and reverse voltages is described by the growing value of the internal integral in Eqn. (1).

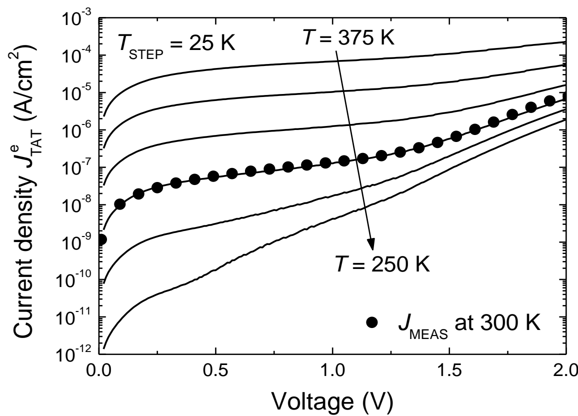

Fig. 2: *Simulated reverse I-V curves of the* metal/GaN/AlGaN *heterostructure at different temperatures.*

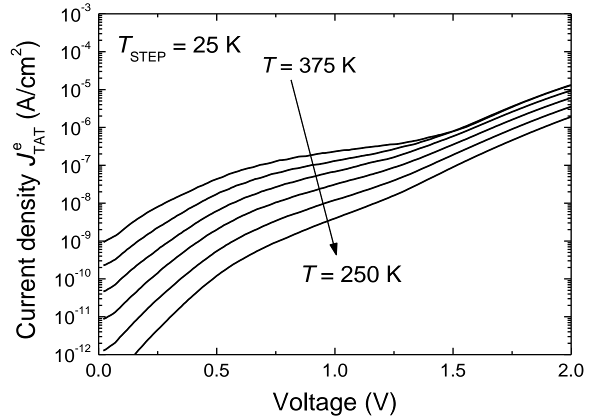

Fig. 3: *Simulated trap-assisted tunnelling current* $J^{\mathrm{e}}_{\mathrm{TAT}}$ *at different temperatures.*

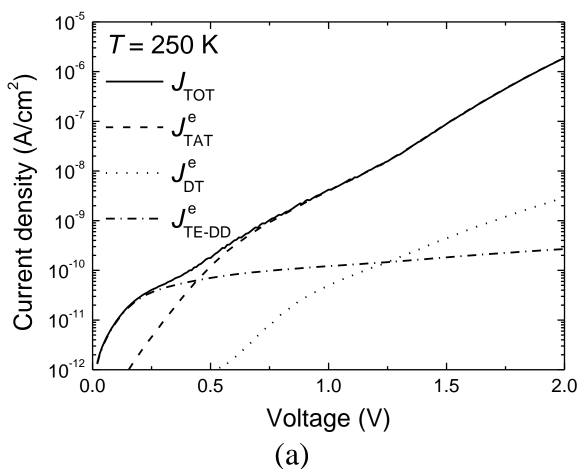

(a)

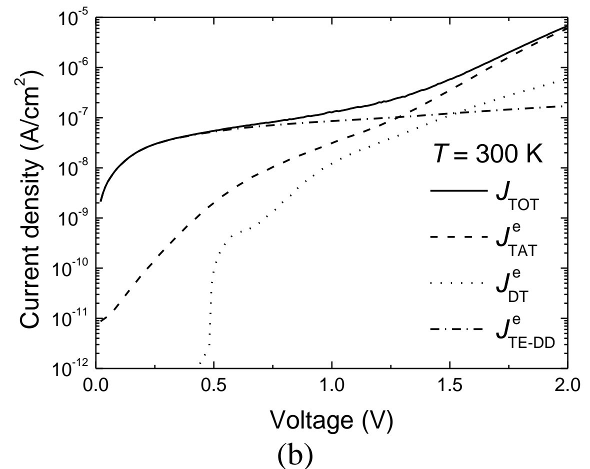

(b)

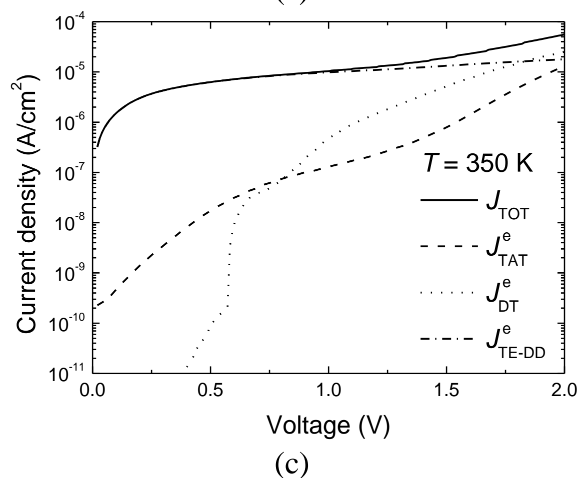

(c)

Figs. 4a,b,c: *Simulated I-V curves of the total current density* $J^{\mathrm{e}}_{\mathrm{TOT}}$, *thermionic-diffusion component* $J^{\mathrm{e}}_{\mathrm{TE\text{-}DD}}(x_{\mathrm{M}})$, *and tunnelling components* $J^{\mathrm{e}}_{\mathrm{DT}}(x_{\mathrm{M}})$ *and* $J^{\mathrm{e}}_{\mathrm{TAT}}(x_{\mathrm{M}})$ *at the place of the* metal/GaN interface x_{M} *at temperatures* 250 K, 300 K *and* 350 K.

5. Conclusion

A model of direct and trap-assisted tunnelling was employed to simulate *I-V* curves of a metal/GaN/Al_XGaN_{1-X}/GaN Schottky heterostructure in the temperature range from 250 K to 375 K. Even though the probability of electron tunnelling is temperature independent, the tunnelling currents depend on temperature because the Fermi-Dirac distribution function occurs in their calculation. Simulations showed that direct tunnelling current J^e_{DT} and termionic-drift-diffusion current $J^e_{TE\text{-}DD}$ are depend on temperature more strongly than trap-assisted tunnelling current J^e_{TAT}, see Fig. 5. This is due to the fact that when calculating the direct tunnelling current the total energy of tunnelling electrons has an unlimited upper limit whereas in the case of trap-assisted tunnelling the total energy of tunnelling electrons is conserved constant.

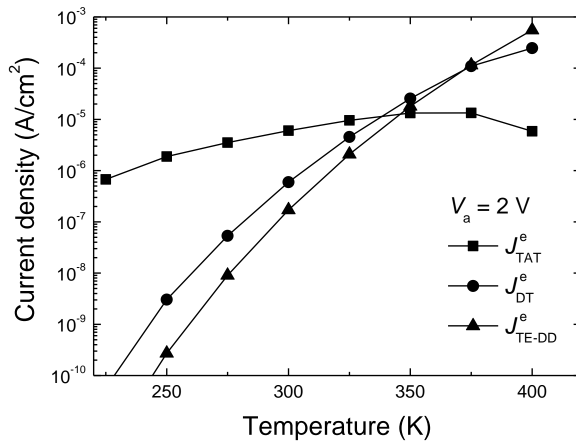

Fig. 5: *Simulated I-T curves of the thermionic-diffusion component* $J^e_{TE\text{-}DD}(x_M)$, *and tunnelling components* $J^e_{DT}(x_M)$ *and* $J^e_{TAT}(x_M)$ *at the place of the* metal/GaN *interface* x_M *at reverse voltage* V_a=2 V.

Acknowledgement

The work has been supported by the Scientific Grant Agency of the Ministry of Education, Science, Research and Sport of the Slovak Republic and of the Slovak Academy of Sciences (projects VEGA 1/0377/13 and VEGA 1/0651/16).

References

[1] J. Racko, P. Valent, P. Benko, D. Donoval, L. Harmatha, P. Pinteš, J. Breza: *Solid-State Electronics*, **52**, 1755 (2008).

[2] J. Racko, P. Benko, I. Hotový, L. Harmatha, M. Mikolášek, R. Granzner, M. Kittler, F. Schwierz, J. Breza: *Applied Surface Science*, **312**, 68 (2014).

[3] J. Racko, P. Ballo, P. Benko, L. Harmatha, A. Grmanová, J. Breza: In: *Proceedings of the International Conference on Applied Physics of Condensed Matter APCOM 2014*, J. Vajda, I. Jamnický (eds.), June 2014, Štrbské Pleso, Slovakia, p. 48 (2014).

[4] J. Racko, P. Benko, L. Harmatha, M. Mikolášek, R. Granzner, M. Kittler, F. Schwierz, J. Breza: In: *Progress in applied surface, interface and thin film science, SURFINT - SREN IV*, 23-26 November 2015, Florence, Italy, p. 124 (2015).